Advances in Geosciences Konstantinos Perakis & Athanasios Moysiadis, Editors
EARSeL, 2012

Observing Coastlines with Satellite Data: a Case Study in Abruzzo (Italy)

Francesco Palazzo[1], Valerio Baiocchi[2], Keti Lelo[2], Maria Vittoria Milone[2], Martina Mormile[2], Andrea Minchella[3], Fabio Del Frate[3], Daniele Latini[3], Sylvie Remondiere[1] and Donatella Dominici[4]
[1] *SERCO SPA, Frascati, Italy; Francesco.palazzo@esa.int; Sylvie.remondiere@serco.com*
[2] *Universitá degli studi di Roma La Sapienza, Dipartimento Ingegneria Civile, Edile ed Ambientale (DICEA), Roma; Valerio.baiocchi@uniroma1.it; Keti.Lelo@gmail.com; mariavittoria.milone@uniroma1.it; martina.mormile@uniroma1.it*
[3] *Universitá degli studi di Roma Tor Vergata, Dipartimento di Informatica, Sistemi e Produzione, Roma, Italy; Andrea.minchella@esa.int; delfrate@disp.uniroma2.it; latini@disp.uniroma2.it*
[4] *Universitá degli studi dell'Aquila, Dipartimento di Architettura ed Urbanistica, L'Aquila, Italy; dominici@dau.ing.univaq.it il*

Abstract. Started in 2009, the COSMOCoast project aims at exploring the potential of satellite data for the retrieval of the instantaneous shoreline. In particular, the focus is on the exploitation of HR and VHR microwave and optical data. Retrieved information, thanks to its potential accuracy in the geolocation and intercompatibility of results can be of interest for analysing coastline variations. To increase the intercompatibility among products acquired with different geometries and in different coastal conditions (low coast and steep coast), are orthorectified and the geolocation accuracy of each outcome product is quantified. Automated extraction of the coastline is carried out (with object oriented and neural network techniques) and the results are compared with the outcome of manual extraction. Differences in the retrieval results at different dates are then analysed in terms of potential inaccuracies in the coastline extraction, meteomarine conditions or other error sources. This paper focuses on the geolocation accuracy estimation of the whole dataset and provides an example of shoreline extraction issues in a complex coastal environment, in the proximity of Vasto, Abruzzo, Italy.

Keywords. Satellite, VHR, shoreline, accuracy.

1. Introduction

Within the last decade, a new generation of satellites with refined observing capabilities in resolution and frequency and often flying in "constellation" were launched and are to be launched. This includes microwave operating systems, such as COSMO-SkyMed, TerraSAR-X/TanDEM-X, the forthcoming Sentinel-1, RADARSAT constellation mission or COSMO-SkyMed second generation, as well as optical payloads such as RapidEye, GeoEye, DigitalGlobe, Pleiades-HR or the forthcoming Sentinel-2. In general, the increased resolution of all those sensors is expected to benefit cartographic applications. In addition, one of the main challenges and perspectives offered by such plethora of sensors and products is the integration of data acquired with different geometries and/or wavelengths, hence densifying the observation timeframe.

The COSMOCoast project, developed by a multi-disciplinary team with a limited funding provided by ASI (contract I/067/09/0), aimed to explore the potential of EO data in support to coastal applications. The generated products might be of interest for the public administration in charge of monitoring of the coastal areas [1].

1.1. Study area

The test area in this project is the coast of Abruzzo, which spans some 130 kilometres NW-SE on the Adriatic sea, central Italy. The coast is representative of different environments from wide, sandy shores, high, jagged cliffs, narrow creeks and pebble beaches. Within the overall test-site, two areas were selected to carry-out detailed ground experiments, one representative of low coast (Pescara) and the other representative of steep coast (Ortona/Vasto).

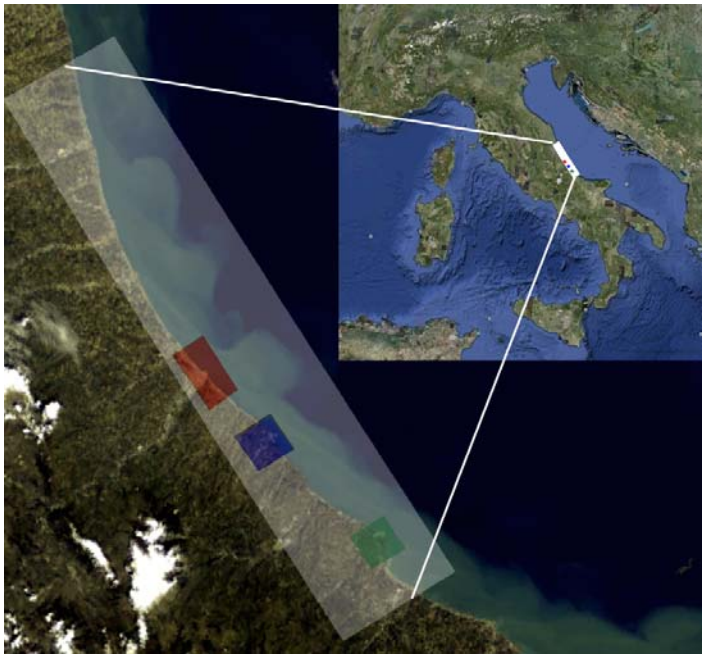

Figure 1: Top right: broad location of the study-areas © Google Earth optical image, bottom left de-tailed location over-imposed to an ENVISAT MERIS image (white: coast of Abruzzo test-site, red: Pescara test site, blue: Ortona test site, green: Vasto test-site).

The reduction of sediment transported to the sea from the main rivers due to creation of dams [2], the increasing human pressure on the coast (from ISTAT data spanning 2002-2011, the overall population increase in coastal municipalities interested by the study is 12%, whereas the trend at regional level is 6%) and the presence of pre-existing structures and infrastructures threatened by their adjacency to the sea has called since the 90's for interventions to protect the coast. Following a first phase during which beach nourishment activities were prevalently implemented, a tendency to intervene with rigid structures (groynes and breakwaters), sometimes jointly with reshaping of the beach has been prevailed. Unfortunately, such interventions seem to have succeeded locally (the number of interventions reported by the municipalities to re-nourish the beach diminished over time), but moved the problem elsewhere, calling for new local interventions. A broad overview of erosion-al/sedimentation trends on larger areas than the ones to be affected by the interventions would probably have helped the various municipalities to better plan and structure the interventions. In addition, the availability of a continuous flow of observations might allow assessing the efficiency of past interventions.

An example of the physical modifications occurred in less than a decade over the Pescara coast is shown in Figure 2: the use of recent (2010/2011) COSMO-SkyMed data allowed updating the in-formation contained in the regional cartography (years 2004-2008) in a scale of 1:5000. Rigid protection structures appearing in the regional cartography (grey), did not obtain the expected

results, as shown by the completely new set of protection works detected with COSMO-SkyMed data (red).

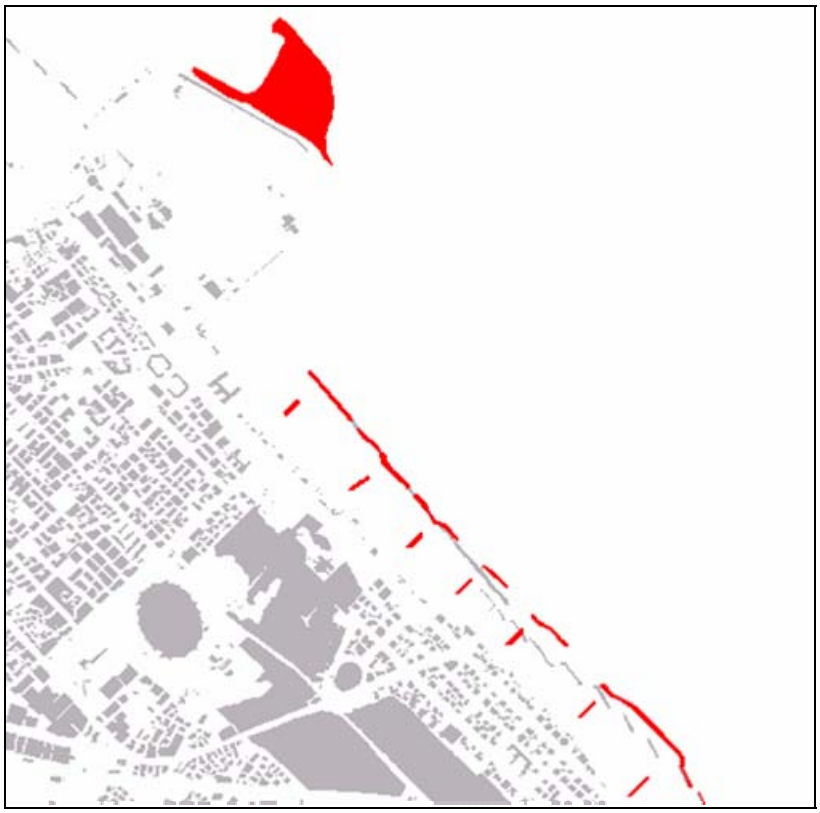

Figure 2: Pescara: former protection works visible on the regional cartography (grey) dating 2004/08 have been removed and re-built in recent years as mapped by COSMO-SkyMed data in 2010/11 (red). North is up.

1.2. The observable

The identification of the boundary land/water on a satellite image acquired at almost nadir conditions may not be difficult (at least in absence of cloud cover in the case of an optical image, or in absence of strong winds and currents in the case of a radar image). However, the understanding of what is observed, and in particular its relationship with the definition of shoreline, is a more complex issue. In fact, only the instantaneous divide between land and water at the time of acquisition can be extracted from an image: this is influenced by local and seasonal meteomarine conditions and only represents one event in time. On the other hand, the definitions of shoreline rely on multi-temporal information, as they refer to an average line over time (e.g. mean high water line, or the zone between mean low water and the upper limit of wave uprush at high tide, or the mean sea level or the chart datum.). An interesting review of some definitions of shoreline is presented in [3]. Such definitions may also vary from a country to another and is also difficult to be applied: e.g. the mean sea level (corresponding to the intersection with the geoid) can be known only in correspondence of fixed measuring stations (mean sea level is defined as the arithmetic mean of hourly water elevations observed over a specific 19-year cycle). In the specific case of Abruzzo, while keeping in mind the intrinsic temporal limit of the line retrievable by the satellite image, it is however possible to try to correlate it to the instantaneous meteomarine conditions, by exploiting the information provided by the Italian National Tidegauge Network, for instance taking into account the planimetric variability related to the different tidal conditions at the date of acquisition [4].

2. Methods

2.1. Data

Several optical products at different ground resolution and wavelengths, IKONOS-2, FORMOSAT-2, KOMPSAT-2 and ORBVIEW-2 have been used. Those products were acquired over two test-sites (Pescara and Ortona) and cover a timespan from 2004 to 2010.

Many radar products acquired at various wavelengths and resolution (L-band: PALSAR, C-band: SAR and ASAR and X-Band: COSMO-SkyMed) have been used. The acquisition dates range from 1993 to 2011, the core of the dataset is represented by 29 COSMO-SkyMed products acquired with different orbital configurations and modes during 2010 and 2011.

COSMO-SkyMed (COnstellation of small Satellites for Mediterranean basin Observation) is the largest Italian investment in Space Systems for Earth Observation, commissioned and funded by Italian Space Agency (ASI) and Italian Ministry of Defense (MoD), and it is conceived as a Dual-Use (Civilian and Defence) end-to-end Earth Observation System. It consists of a constellation of four Low Earth Orbit mid-sized satellites, each equipped with a multi-mode high-resolution Synthetic Aperture Radar (SAR) operating at X-band. Amongst the various available acquisition modes, Enhanced Spotlight products and Stripmap mode Himage products were used. Enhanced Spotlight products have an azimuth frame extension of about 11 km, a range swath extension of about 11 km, with a ground resolution, both in range and azimuth of less than 1 m. Stripmap mode Himage products have a swath width of about 40 km, an azimuth extension of about 40 km, with a ground resolution, both in range and azimuth of less than 3 m. More information about COSMO-SkyMed can be found in [5]. The availability of up to 2 observations per day allowed the project to plan acquisitions close in time to specific tidal events (e.g. low tide, high tide or 0 tide).

Table 1. List and properties of the (V)HR recent products used by the project (CS=Cosmo-SkyMed; ASC=Ascending, DES=Descending, PAN=Panchromatic, MS=Multispectral, HH=Horizontal/Horizontal, VV=Vertical/Vertical).

Product	Date	Time	Angle	Comments
IKONOS-2	07-01-2004	10:13	16	PAN (0.45-0.90), MS(0.445-0.516; 0.506-0.595; 0.632-0.698; 0.757-0.853)
IKONOS-2	29-01-2004	10:15	13	PAN (0.45-0.90), MS(0.445-0.516; 0.506-0.595; 0.632-0.698; 0.757-0.853)
IKONOS-2	28-06-2007	10:02	19	PAN (0.45-0.90), MS(0.445-0.516; 0.506-0.595; 0.632-0.698; 0.757-0.853), 2 adjacent products
CS Stripmap	26-12- 2009	04:51	23	ASC, Right view, HH Polarisation, 3 adjacent products
WORLDVIEW-2	29-06-2010	10:05	9	PAN (0.45-0.8), MS(0.400-0.450; 0.450-0.510; 0.510-0.580; 0.585-0.625; 0.630-0.690; 0.705-0.745; 0.770-0.895; 0.860-1.040)
CS Spotlight	06-06-2010	04:01	45	ASC, Left view, HH Polarisation
CS Spotlight	06-07-2010	04:49	24	ASC, Right view, HH Polarisation
CS Spotlight	07-07-2010	04:01	45	ASC, Left view, HH Polarisation
CS Spotlight	07-07-2010	16:54	49	DES, Right view, HH Polarisation
CS Spotlight	09-07-2010	04:07	40	ASC, Left view, HH Polarisation
CS Spotlight	10-07-2010	05:13	48	ASC, Right view, HH Polarisation
CS Spotlight	10-07-2010	17:00	45	DES, Right view, HH Polarisation

Product	Date	Time	Angle	Comments
CS Stripmap	15-07-2010	04:49	22	ASC, Right view, HH Polarisation, 2 adjacent products
CS Spotlight	15-07-2010	16:54	55	DES, Right view, VV Polarisation
KOMPSAT-2	17-07-2010	08:37	13	PAN (0.50-0.90), MS(0.45-0.52; 0.52-0.60; 0.63-0.69; 0.76-0.90), 2 adjacent products
FORMOSAT-2	19-07-2010	08:40	45	PAN (0.45-0.90), MS(0.45-0.52; 0.52-0.60; 0.63-0.69; 0.76-0.90)
FORMOSAT-2	21-07-2010	08:40	45	PAN (0.45-0.90), MS(0.45-0.52; 0.52-0.60; 0.63-0.69; 0.76-0.90)
CS Stripmap	29-12-2010	04:47	25	ASC, Right view, HH Polarisation, 3 adjacent products
CS Stripmap	31-12-2010	17:10	32	DES, Right view, HH Polarisation
CS Spotlight	14-05-2011	04:46	23	ASC, Right view, HH Polarisation
CS Spotlight	25-07-2011	04:45	23	ASC, Right view, HH Polarisation
CS Spotlight	26-07-2011	05:03	44	ASC, Right view, HH Polarisation
CS Stripmap	27-07-2011	04:57	43	ASC, Right view, HH Polarisation, 3 adjacent products
CS Stripmap	31-07-2011	04:57	47	ASC, Right view, HH Polarisation
CS Spotlight	28-07-2011	04:51	32	ASC, Right view, VV Polarisation
CS Spotlight	29-07-2011	04:51	37	ASC, Right view, HH Polarisation
CS Spotlight	01-08-2011	04:09	36	ASC, Right view, HH Polarisation
CS Spotlight	23-11-2011	17:13	27	DES, Right view, HH Polarisation
CS Spotlight	05-12-2011	17:12	23	DES, Right view, HH Polarisation

In addition, dedicated ground campaigns were carried with GNSS geodetic differential surveys, kinematic GPS and with a Ground Lidar acquisition, in order to collect data as ground control points and validate the results. A high resolution DEM (2 m pixel size) was generated by the project based on regional cartography and meteomarine observations collected by the Italian National Tidegauge Network were available to the team.

2.2. Methods

From Table 1 it is clear that the satellite acquisitions were taken with various off-nadir angles at the scene center and at different orbital configurations. This results in geometric distortions that needs to be taken into account when trying to compare different data. This problem is shown in Figure 3 for the case of radar data acquired by the same sensor with different acquisition geometries. To enhance comparability among data, all products were orthorectified, even if this does not solve lack of information in presence of particular orbital configurations and ground terrain morphologies (shadows).

Figure 3: Left: COSMO-SkyMed acquisition taken in Right-Ascending mode -product COSMO-SkyMed © ASI (2011). Right: The same areas imaged by a COSMO-SkyMed acquisition in Right-Descending mode -product COSMO-SkyMed © ASI (2011). Differences in the illumination of walls/roofs and fields are evident. The dune system (white area in the upper section of the images) does not seem particularly affected by the change in illumination direction, probably due to its roughness.

Since estimated accuracy of the instantaneous land-water border depends on the resolution of the images, the model adopted, the accuracy of Ground Control Points (GCP) and the DEM available, all such inputs were carefully analysed.

For shoreline extraction from optical data, it is well known that multispectral information can provide useful information for the discrimination between land and water [6], [7], [8], however the spatial resolution of the available products is generally low (4 m for IKONOS-2 and KOMPSAT-2, 8 m for FORMOSAT-2). The multispectral bands were then fused in order to benefit from the higher spatial resolution from the panchromatic band.

Most of the authors [9], [10], [11] believe that the photogrammetric rigorous model of orthorectification is the best choice when orbital metadata and enough ground control points (GCP's) with proper accuracy are available. This is for two main characteristics of these models: their accuracy and their robustness. Positioning accuracy of these models is considered in literature the best achievable, up to half a pixel of the raw image. This accuracy is due to the geometric, optical and physical reconstruction of the acquisition phase performed by such models based on the well-known collinearity equations. This characteristic is also due to their robustness; these models are not very sensible to outliers. Only Rapid Positioning Coefficient (RPC) models have characteristics similar to Rigorous orbital modelling because they are based on the orbital characteristics of the acquisition but with a simplified approach: their only advantage compared to rigorous models is that they need less GCPs, sometimes two or three may be enough while rigorous model requires anyway more than six or eight GCPs. The rigorous model was therefore applied to the optical imagery when possible, even if in earlier experimentations it was observed that sometimes orbital rigorous models can show some instability probably due to the alignment of GCPs along the coast-line that can be considered as a straight line [12]. In the case of radar data, the Range Doppler method [13] was applied on complex COSMO-SkyMed images. This uses available orbit state vector information in the metadata, radar timing annotations, slant to ground range conversion parameters together with the reference DEM data to derive the precise geolocation information.

To be sure that the GCPs may be used on all the optical and radar images, they were acquired on "natural" details that may be considered stable during all years covered by the imagery. So, collimable and surveyable points were chosen such as corner of buildings, roads or sidewalks

and other stable and visible features present on ground. When possible, points were differentiated both with real time and post processing techniques to avoid outlier and for the same reason, 20% of the points were surveyed two times in different days. On Pescara site, a density of 1 point every 5 km^2 was used as guideline; this density is surely redundant for a single image but it was observed during this and precedent research that not all the point collimable on a specific images are recognizable on other images also if they have greater resolution. For Ortona test site, more than twenty GCPs were acquired and a similar ground campaign has been carried out. Pescara site was acquired using only GPS satellites while Ortona site survey used also Glonass constellation. In both cases, a post processing elaboration was performed and referred to official GPS stations managed by "Regione Abruzzo" (Regional administration of Abruzzo), so that all points are referred to official national reference IGM95-ETRF89. The ellipsoidal height measured by GNSS survey was converted in orhometric heights using ITALGEO05 geoid model that has a stated accuracy of +/-2 cm.

3. Results

3.1. Accuracy assessment

The high resolution DEM generated from the cartographic production and used for othorectification of optical and radar data was compared with points taken by GPS and related to the areas of Pe-scara and Ortona, in order to estimate its accuracy level. This resulted in the vertical accuracy reported in Table 2. An extensive validation area was not within the goal of the project; however the local point's estimates can give an overall idea of the average quality of the DEM.

Table 2. Estimation of the DEM accuracy.

Parameter	Cartographic DEM
Average (m)	1.4371
Median (m)	1.1624
σ (m)	1.2062

Accuracy and precision of the orthorectified optical images were then assessed. The analysis was performed by carrying out several tests on each image, by varying the number of Ground Control and Check Points. As shown in Figure 4, all the values of North and East RMS estimated for the GCPs tend to match the pixel size, hence the achieved precision is of the order of the pixel. RMS values estimated for CPs are shown to be 1.5 times the pixel size: as the value is lower than 2 pixels, the achievable accuracy for each image seems satisfactory.

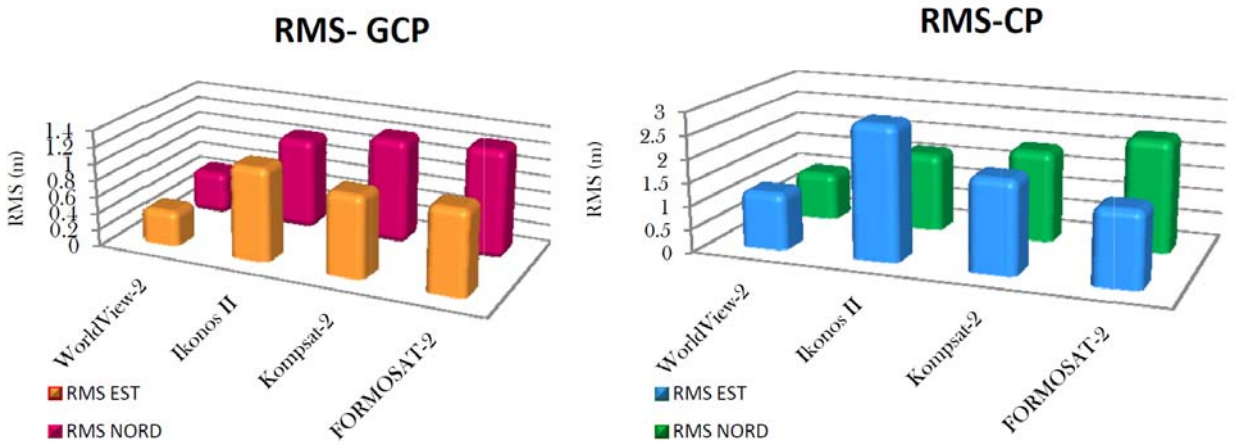

Figure 4: Left RMS estimated for the GCPs; Right: RMS estimated for the CPs.

A similar analysis carried out on the COSMO-SkyMed dataset showed that the reachable geolocation accuracies range in the case of Spotlight products are among 1 and 4 meters, whereas in the case of Stripmap products it varies from 3 to 8 m. The areas showing the worst geolocation are the ones characterised by the steepest slopes or by the presence of image artifacts.

Accuracies of the coastlines extracted automatically (radar) and semi-automatically (optical) have been compared with manually extracted coastlines and, for what concerns radar data, are being presented elsewhere [14].

3.2. The impact of DEM quality on results

The project produced coastlines at various resolution, date and geographic extension using data listed in Table 1 and explored the advantages and new frontiers offered by VHR satellite data compared to HR data (eg ERS SAR, ENVISAT ASAR and ALOS PALSAR). In this paragraph, we present an example of the issues that were faced during the shoreline extraction process in the area of Vasto, Abruzzo, using only radar data.

This is an area characterised by a continuous transition from low coast to steep riffs, within a complex reef environment, parallel to the coast. The investigated area has an extension of about 10km, out of which an aggregated total of 3km present very steep slopes (>30 up to sub-vertical) near the boundary land/sea. The area was selected to test the feasibility of shoreline extraction in "extreme" conditions. For this purpose, radar acquisitions were taken within different seasonal conditions (summer vs winter) and with different acquisition geometries (right descending vs right ascending). The steep coast and the reef in fact challenge the efficiency of shoreline extraction, as several areas of shadow/layover/foreshortening might exist, based on acquisition geometry. Selection of different acquisition geometries may help attenuating the problem related to the missing information.

Figure 5 shows the output of the comparison between shorelines extracted from acquisitions taken in different acquisition geometries.

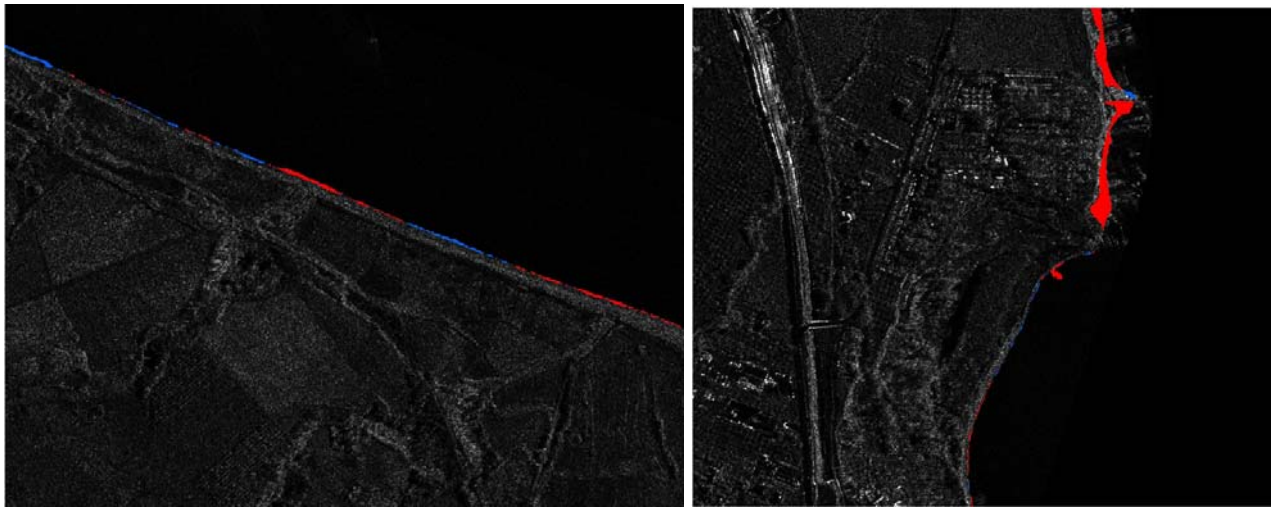

Figure 5: Seasonal variations in the location of the shoreline for the Vasto test-area: red "erosion", blue "sedimentation". Differences in the left inset range within the limits of normal variability associated to meteomarine factors (eg tidal differences at the acquisition dates). The red part on the right inset appears instead related to other issues, with an average discrepancy between summer/winter shoreline of some 20 meters. Interestingly, the lower part of the same inset shows no variations between the two dates. Background product COSMO-SkyMed © ASI (2011). North is up.

Given the very short time interval between acquisitions and the different seasonal conditions, the specific experiment was not conceived to quantify the rate of change or identify processes, but only to test applicability and sensitivity of the data to a challenging environment. The larger differences identified in the area (>10 m) are independent from meteomarine conditions (areas of the images with the same geomorphologic configuration and orientation should present similar differences, and this is not the case) and are above the planar discrepancies implied by a 0.17 m tidal height difference (10 m for a 1o slope) at the 2 acquisition dates, given the average steepness of the coast. In the attempt to identify the source of such discrepancies, the various level of processed data were then intercompared, also with optical "ground truth".

Figure 6: Left: orthorectified image -product COSMO-SkyMed © ASI (2011), Center: source image (reprojected without DEM to facilitate comparison) -product COSMO-SkyMed © ASI (2011) and Right: optical image of the same area © Google Earth optical image. The shoreline can be easily traced on the reprojected image, whereas in the case of the orthorectified image there appear to be artifacts.

Such comparison is shown in Figure 6, which refers to the same location presented in the right inset of Figure 5. The figure presents a right descending radar acquisition (this should limit shadows

generated from the inland, but might be susceptible to backscattering created by the reef), processed as a high level output (orthorectified with the high resolution DEM), as source image (reprojected on ground range without DEM) and the corresponding optical image. Several artifacts in the orthorectified image are clearly visible.

A closer comparison of the used DEM with the processed data, allowed to locate the problem areas and to see how they relate to local errors in the DEM. It seems that several parallel reefs were extracted by the DEM photointerpreters, as land areas and assigned to different contour line values. In the orthorectification process this resulted in the erroneous stretching of the reefs, interpreted from the DEM as land. Reprocessing the radar images with the SRTM DEM removes the problem, but may induce additional geolocation issues, due to the coarser resolution (and vertical accuracy) of the DEM in such steep areas.

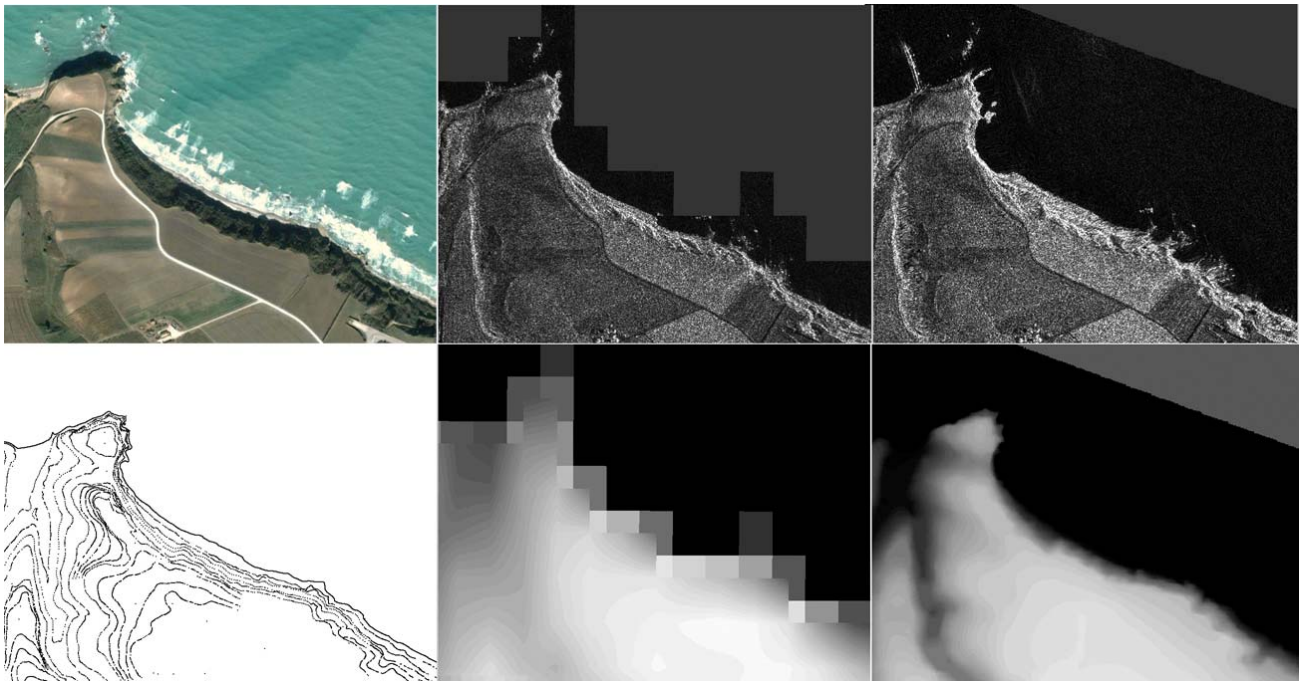

Figure 7: Cape Aderci. Top row, from left to right: optical image © Google Earth, COSMO-SkyMed image orthorectified with the SRTM DEM and the same image orthorectified with the high resolution DEM generated from the regional cartography. Bottom row, from left to right: regional cartography, SRTM DEM (the coarse pixel size can be seen) and high resolution DEM. Red circles: artifacts created by the DEMs. Red arrow: similarity in the morphology presented by the regional cartography and the area where waves break. North is up.

Another example for the same type of problem can be documented for cape Aderci. Also in this case the coastal morphology identifiable in the image processed with the high resolution DEM, presents strange features. This is shown in Figure 7, where the orthorectified image with the high resolution DEM (right inset) shows at least 2 unnatural features. The image used in this example is a right ascending summer radar acquisition. A lower speckle effect on the water area compared to the winter acquisitions of Figure 6 can also be noticed: this is due to a 1.7 m/s wind speed documented for this acquisition, much lower than the 7.0 m/s wind speed for the winter acquisition. Also in this case it is very likely that the photointerpreters extracting the contours from aerial photographs to generate the regional cartography interpreted areas of breaking waves as land and erroneously assigned to them height values. The problem can be illustrated clearly with the non-nadiral satellite acquisition of the area shown on the left inset of Figure 7. This scene is derived from Google Earth and provides a potential example of “pseudo” aerial photograph (taken in roll/tilt conditions –probably due to strong winds- with varying geometry) acquired in non-optimal

conditions. Shadows and meteomarine conditions in fact compromise the identification of the shoreline. By a comparison with the morphology shown by the contour lines used to create the high resolution DEM, there seems to be some similarity between the area of wave breaking and the "0 height" con-tour. Also the orthorectified image with the SRTM DEM (centre inset in Figure 7), that appears to be more similar to the morphology presented by the optical image, shows one problematic area. This corresponds to the junction between three DEM pixels of very different value, the problem could probably be smoothened (but not removed) in the orthorectification process by using a higher order DEM interpolator.

An estimate of the extension of the areas interested by the large discrepancies illustrated in Figure 5 indicates that this is affecting 11% of the considered coast. Almost in all cases, the areas with errors correspond to zones of steep cliffs or reefs presenting a discrepancy between the morphology depicted by satellite acquisitions (independently from the acquisition geometry) and the contour lines.

Based on all the previous observations it might be concluded that availability of a high resolution, high quality (recent) and thoroughly validated DEM is essential to avoid creation of additional uncertainties in shoreline extraction and comparison in steep coastal areas.

4. Conclusions

In general, the achieved geolocation accuracy within the analysed VHR dataset (optical and radar) appears comparable, therefore a monitoring system based on observations taken by sensors acquiring with different observation geometries or different bands appears feasible. Distortions related to morphology, as well as absence of information in areas of shadow may affect the overall quality and comparability of the results, and these are more likely to happen in areas of high coast, characterised by a reef system parallel to the coast.

Areas of low coast are expected to show a large variability in the planimetric location of the shore-line, as a consequence of the different meteomarine conditions. When considering the sources of inaccuracy in the location of the extracted shoreline, the bias induced by geolocation inaccuracy in areas of high coast may turn out to be of similar entity to the bias induced by the meteomarine conditions in the areas of low coast, in absence of additional error sources. The importance of the availability of an up to date and accurate DEM has been highlighted in this contribution. The project has now been successfully completed, however the large amount of material produced is still being analysed.

Acknowledgements

This research was carried out within the framework of an ASI contract (I/067/09/0). COSMO-SkyMed data were provided by ASI (AO project 1560), IKONOS, ALOS, KOMPSAT-2, FORMOSAT-2. ERS data were provided by the European Space Agency (C1P 6894 and C1P 4592).

References

[1] Palazzo, F., Latini, D., Baiocchi, V., Del Frate, F., Giannone, F., Dominici, D., Remondiere, S., 2012. An application of COSMO-SkyMed to coastal erosion studies. *European Journal of Remote Sensing*.

[2] Venturini, G., Visca, C., Caputi, P., De Girolamo, P., D'Alessandro, L., Mascioli, F., 2008. Strategie di gestione integrata dell'area costiera: le azioni intraprese dalla Regione Abruzzo. Atti del convegno Coste: Prevenire, Programmare, Pianificare, Autorità di Bacino della Basilicata.

[3] Boak, E. H., Turner, I. L., 2005. Shoreline Definition and Detection: A Review. *Journal of Coastal Research*: Volume 21, Issue 4: pp. 688 – 703.

[4] Palazzo, F., Baiocchi, V., Del Frate, F., Giannone, F., Dominici, D., Latini, D. and Remondiere, S., 2011. Remote Sensing as a Tool to Monitor and Analyse Abruzzo Coastal Changes: Preliminary Results from the ASI COSMO-Coast Project. *5th EARSeL Workshop on Remote Sensing of the Coastal Zone Proceedings*, Prague.

[5] Italian Space Agency COSMO-SkyMed Mission COSMO-SkyMed System Description & User Guide, 46 pages, available online at: http://www.eurimage.com/products/pdf/csk-user_guide.pdf, last visited: 4 April 2012.

[6] Mc Feeters, S. K., 1996. The use of normalized difference water index (NDWI) in the delineation of open water features. *International Journal of Remote Sensing*, 17, pp.1425–1432.

[7] Xu, H., 2006. Modification of normalised difference water index (NDWI) to enhance open water features in remotely sensed imagery. *International Journal of Remote Sensing*, 27:14, pp. 3025-3033.

[8] Lyzenga, D. R., Malinas, N. P., Tanis, F. J., 2006. Multispectral Bathymetry Using a Simple Physically Based Algorithm. *IEEE Transactions on Geoscience and Remote Sensing*, Vol.44, No.8, pp. 2251-2259.

[9] Baiocchi, V., Crespi, M., De Vendictis, L. and Giannone, F., 2004. Utilizzo di immagini satellitari ad alta risoluzione per scopi metrici. *Atti VIII Conferenza ASITA*, Roma 14-17 dicembre 2004.

[10] Gruen, A. and Zhang, L., 2002. Automatic DTM Generation from Three-Line-Scanner (TLS) images. *IAPRS*, Vol. 34, Part 2A, Graz, Austria, pp. 131-137.

[11] Toutin, T., 2004. Review article: Geometric processing of remote sensing images: models, algorithms and methods. *International Journal of Remote Sensing*, 25, pp.1893-1924.

[12] Baiocchi, V., Del Guzzo, F., Dominici, D. and Lelo, K., 2007. Comparative methods for the extraction of coastal areas from VHR images, *Proceedings 27th EARSeL Symposium*, 7-9 June Bolzano, Italy.

[13] Small, D. and Schubert, A., 2008. *Guide to ASAR Geocoding*. RSL-ASAR-GC-AD, Issue 1.0.

[14] Latini, D., Palazzo, F., Del Frate, F. and Minchella, A., 2012. Coastline extraction from SAR COSMO-SkyMed data using a new neural network algorithm, accepted to *IEEE Proceedings of IGARSS 2012*, Munich.